

See discussions, stats, and author profiles for this publication at: <https://www.researchgate.net/publication/29860141>

Incoherent Electron–Phonon Scattering in Octanethiols

ARTICLE *in* NANO LETTERS · SEPTEMBER 2004

Impact Factor: 13.59 · DOI: 10.1021/nl048841h · Source: OAI

CITATIONS

89

READS

62

6 AUTHORS, INCLUDING:



A. Pecchia

Italian National Research Council

109 PUBLICATIONS **1,198** CITATIONS

SEE PROFILE



Aldo Di Carlo

University of Rome Tor Vergata

485 PUBLICATIONS **7,111** CITATIONS

SEE PROFILE



Thomas Frauenheim

Universität Bremen

368 PUBLICATIONS **12,028** CITATIONS

SEE PROFILE



Rafael Gutierrez

Technische Universität Dresden

89 PUBLICATIONS **1,410** CITATIONS

SEE PROFILE

Incoherent Electron–Phonon Scattering in Octanethiols

Alessandro Pecchia* and Aldo Di Carlo

*INFN–Dipartimento di Ingegneria Elettronica, Università di Roma “Tor Vergata”,
Via del Politecnico 1, Roma 00133, Italy*

Alessio Gagliardi, Simone Sanna, and Thomas Frauenheim

*Institute for Theoretical Physics, University of Paderborn,
D-33098 Paderborn, Germany*

Rafael Gutierrez

*Institute for Theoretical Physics, University of Regensburg,
D-93040 Regensburg, Germany*

Received July 21, 2004; Revised Manuscript Received September 8, 2004

ABSTRACT

We investigate the influence of molecular vibrations on the tunneling of electrons through an octane–thiolate sandwiched between two gold contacts. The coherent and incoherent tunneling currents are computed using the non-equilibrium Green's functions formalism. Both the system Hamiltonian and the electron–phonon interaction are obtained from first-principles DFT calculations, including a microscopic treatment of the gold contacts. This method allows to study explicitly the influence of each individual vibrational mode and show a detailed analysis of the power dissipated in the molecular wire.

The emerging field of molecular electronics has seen a tremendous expansion in recent years, thanks to the development of new experimental techniques^{1,2} which have allowed to achieve trusted and reproducible results. The use of organic material in electronic devices represent an interesting technology in its own right for the unique possibilities it offers.³ Organic structures can exploit the richness of the organic chemistry, resulting in a number of specific functionalities that are well suited for sophisticated sensors with a high degree of selectivity for gas, biochemical, and lab-on-a-chip applications. Molecular design could also be exploited for band engineering that could be applied to nanoelectronics.

Electronic conduction through a variety of different molecules has been studied experimentally by many research groups,^{4–7} and novel design architectures for memories and logic circuits involving single molecules as active components have been explored.^{8,9} Temperature-dependent transport and power dissipation in molecular devices is necessarily a problem that device design will need to face in the future. To our knowledge, only few works have dealt with this issue in recent years.^{10,11} In recent months there has been a growth of experiments probing the electron–phonon interaction in molecular transport.^{12,13} These experiments are essentially inelastic electron tunneling spectroscopy (IETS) measure-

ments, probing directly the strength of the inelastic electron–phonon scattering. Such type of inelastic mechanisms are mainly responsible for thermal relaxations in molecular junctions, and understanding these mechanisms is important for controlling molecular stability. Furthermore, electron–phonon scattering may provide paths for molecular isomerization, which is useful for switching mechanisms.

Although a simple and clear understanding of transport mechanisms has not been reached yet for most of the molecular compounds, transport in alkenethiols is essentially at a mature stage of experimental development. Such type of molecules align on Au surfaces via covalent S–Au bonds to form regular and stable self-assembled monolayers (SAMs). They are characterized by a large optical band gap (>5 eV), making them very stable to photodegradation. The same large gap is responsible for a very low conduction via tunneling in Au/thiol/Au structures, giving good electrical stability. For the reasons above, it is not surprising that experiments of conduction through these compounds have been reproduced by many research groups.

In this paper we examine the incoherent component of the tunneling current through alkeno–thiolate molecules^{14,15} between gold contacts.

The electronic system is described via a local basis density functional scheme, where appropriate approximations are

* Corresponding author. E-mail: pecchia@ing.uniroma2.it.

considered in order to make the approach efficient for systems comprising large numbers of atoms.^{16–18} The most important are the use of an optimized minimal basis set and the neglect of three-center integrals. The ionic potential is obtained under the standard Born–Oppenheimer approximation. The delicate repulsive part of the potential is expressed as a superposition of atomic pair potentials that are obtained from *ab initio* DFT reference calculations.¹⁸ The method has been recently extended to non-equilibrium quantum transport calculations.^{19,20} A version of this code (gDFTB) is available online.²¹ This method has proven to be successful when applied to organic molecules, giving vibrational frequencies close to experimental results and similar in quality to sophisticated and time-consuming full *ab initio* calculations.^{22,23}

The usual procedure to treat molecular vibrations is to expand the effective nuclear potential up to the harmonic term, and to decouple the Hamiltonian as a superposition of independent one-dimensional oscillators corresponding to the normal modes of vibrations. Each vibrational mode will be labeled by q . The harmonic oscillators can be quantized following the usual prescriptions, by making use of the standard relationships between the position operator and the Bose field operator.

Inelastic electron–phonon scattering in molecular wires has been so far analyzed using model Hamiltonians.^{24–28} In this paper we report the first attempt to study the electron–phonon coupling in a realistic molecular system by explicitly taking into account the molecular degrees of freedom and analyzing in detail the contributions of the vibrational modes. The electronic deformation potential is obtained by expanding the Hamiltonian to first order in the atomic displacements. Subsequently, the atomic coordinates are expressed as a superposition of creation–annihilation operators, a_q^+ and a_q , of phonon quanta in each vibrational mode q . The result is a term in the Hamiltonian describing the electron–phonon coupling,

$$H_{\text{el-ph}} = \sum_{q\mu,\nu} \gamma_{\mu\nu}^q c_\mu^+ c_\nu [a_q^+ + a_q] \quad (1)$$

where c_μ^+ and c_ν are, respectively, the creation and annihilation operators of one electron in the local basis and

$$\gamma_{\mu\nu}^q = \sqrt{\frac{\hbar}{2\omega_q M_q}} \sum_\alpha \left[\frac{\partial H_{\mu\nu}}{\partial R_\alpha} - \sum_{\sigma,\lambda} \frac{\partial S_{\mu\sigma}}{\partial R_\alpha} S_{\sigma\lambda}^{-1} H_{\lambda\nu} - \sum_{\sigma,\lambda} H_{\mu\lambda} S_{\lambda\sigma}^{-1} \frac{\partial S_{\mu\nu}}{\partial R_\alpha} \right] \mathbf{e}_\alpha^q \quad (2)$$

are the electron–phonon coupling matrices. M_q are the atomic masses, ω_q the mode frequencies, and \mathbf{e}_α^q are the normalized atomic displacements for each mode. The non-orthogonality of the basis set is reflected by the presence of the overlap matrix, $S_{\mu\nu}$, and its derivative with respect to the ionic positions, R_α . Therefore, the ionic vibrations of a molecular wire can be described as a class of boson particles which are here referred to as “phonons”.

While crossing the system, the electrons interact with the molecular ionic vibrations from which they can be inelastically scattered. In the present context we assume that the metal ions do not move; henceforth, the electron–phonon scattering within the leads is neglected. This is a good approximation given the very large difference in atomic masses between the Au atoms and the organic elements. Furthermore, we are specifically interested in the energy dissipated within the molecular degrees of freedom, since the inelastic electron–phonon scattering in the metallic leads is known to be small and not important for power dissipation issues. The present method neglects the coupling between contact and molecular modes. Indeed, a degree of mixing between the acoustic modes of the metal and the low energy molecular modes can be expected. In principle, such coupling can be included in the formalism.

Generally speaking, the equilibrium perturbation theory is not suitable to describe the properties of a system driven out of equilibrium by an applied bias. The resulting net flux of current sustained by the bias is an evidence that the system is not in equilibrium. In particular, the equilibrium theory fails to describe real exchange of energy between the electron and the phonon subsystems, and therefore it is unsuitable to describe joule heating and dissipation. This is obvious since in equilibrium there cannot be a steady flux of energy from the electron system to the vibrational degrees of freedom. The generalization of the equilibrium many-body perturbation theory to non-equilibrium is obtained by the Keldysh–Kadanoff–Baym (KKB) formalism.^{29,30} The technicalities of the theory are mathematically rather involved and we refer the reader to specialized reviews which can be found, for example, in ref 32. In the complete non-equilibrium Green’s function approach the electron–vibration interaction is described via both virtual and real emission and absorption of phonon quanta.

The current is computed using a generalized version of the Landauer formula, valid also for non-equilibrium conditions and in particular when sources of incoherent scattering are present. In the steady-state limit, this reads as

$$I = \frac{2e}{h} \int_{-\infty}^{+\infty} \text{Tr}[\Sigma_L^<(\omega)G^>(\omega) - \Sigma_L^>(\omega)G^<(\omega)] d\omega \quad (3)$$

where $\Sigma_L^{<(>)}$ represents the in-scattering of electrons (holes) through the *left* contact of the device, while $G^{<(>)}$ is the electron (hole) correlation function, which essentially represents the density of occupied (empty) states. Current conservation ensures that the same result is obtained when the *right* contact is used instead. The physical interpretation of eq 3 is a simple balance between incoming electrons into empty states and incoming holes into occupied states, equivalent to outgoing electrons from occupied states. The correlation functions, $G^<$ and $G^>$, are related to the in(out)-scattering functions by the standard KKB kinetic equations,^{29,30} given by

$$G^{<(>) }(\omega) = G^r(\omega) \Sigma^{<(>) }(\omega) G^a(\omega) \quad (4)$$

The two lesser and greater self-energies (SE) are the sum of three terms:

$$\Sigma^{(>)}(\omega) = \Sigma_L^{(>)}(\omega) + \Sigma_R^{(>)}(\omega) + \Sigma_{\text{ph}}^{(>)}(\omega) \quad (5)$$

The first two contributions come from the contacts and the third term is related to the scattering processes within the molecule caused by electron–phonon interactions. Such decoupling is valid within the noncrossing approximation (NCA), which we took care to fulfill by physically separating the molecular subunit, free to move, from the contacts. Such separation was obtained with three layers of Au atoms representing the metal surfaces that have been treated as to be part of the molecular region. Because of the short range of the atomic orbital interactions and since the Au atoms do not move, such three layers ensure that the contact and electron–phonon self-energies act on orthogonal subspaces of the Hamiltonian matrix. Combining equations 3, 4, and 5, it is possible to separate the coherent from the incoherent contributions to the total current. These can be written as

$$I_{\text{coh(inc)}} = \frac{2e}{h} \int_{-\text{inf}}^{+\text{inf}} \text{Tr}[\Sigma_L^{<}(\omega) G^r(\omega) \Sigma_{R(\text{ph})}^{>}(\omega) G^a(\omega) - \Sigma_L^{>}(\omega) G^r(\omega) \Sigma_{R(\text{ph})}^{<}(\omega) G^a(\omega)] d\omega \quad (6)$$

The relevant self-energy due to electron–phonon scattering is evaluated within the Born approximation (BA), which is translated into an analytic form by using the standard rules of Feynman’s diagrams and the Langreth theorem for the analytic continuation rules of the Keldysh Green’s functions:

$$\Sigma_{\text{ph}}^{(>)}(\omega) = i \sum_q \gamma_q^2 \int_{-\text{inf}}^{+\text{inf}} \frac{d\omega'}{2\pi} G^{<(>)}(\omega - \omega') D_q^{<(>)}(\omega') \quad (7)$$

where $D_q^{<(>)}$ are the correlation functions related to the vibrational modes. In the actual calculations the zero-th order phonon propagator are used. In principle, the exchange of energy between molecular phonon and thermal bath could be included explicitly by solving an additional kinetic equation. Such an approach is relevant in studying heat dissipations into the contacts.

Equation 7 is usually solved just to first-order, using the unperturbed $G_0^{<(>)}$ functions, obtained from eq 4 by setting $\Sigma_{\text{ph}}^{<(>)} = 0$. This is commonly called first-order BA. However eqs 7 and 4 can be solved in a self-consistent manner (SCBA).³¹ This corresponds to a partial summation of diagrams that goes beyond the simpler first order approximation. A self-consistent solution is computationally far more demanding but leads to a result that is more satisfactory from a theoretical point of view. Only the self-consistent solution, in fact, preserves the contact current in eq 3, which is generally violated when using the simpler first-order BA.

In self-consistent calculations the retarded (advanced) $G^{r(a)}(\omega)$ Green’s functions that appear in eq 4 are, in principle, the exact GF of the electron–phonon coupled

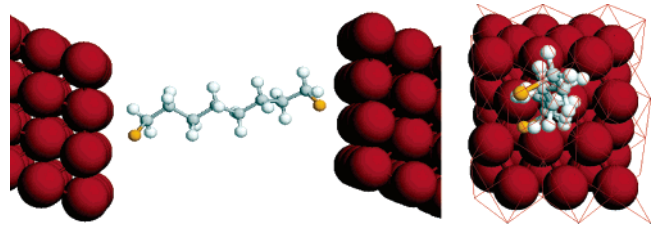


Figure 1. Diagram representing the relaxed atomic coordinates of the octanedithiol between Au contacts.

system and should be renormalized with a corresponding electron–phonon self-energy. In general, the electronic self-energy can be calculated from explicit applications of the Langreth evaluation rules of the non-equilibrium Feynman diagrams. Explicit expressions can be found, for instance, in ref 20. Since we are mainly interested on incoherent phonon emission, we approximate the phonon self-energy to be purely imaginary, neglecting the shift of the van-Hoove singularities (i.e., essentially neglecting energy shifts due to polaron-like states). This assumption is valid since the molecular levels are far from the relevant range of injection energies and therefore the small shift will not modify appreciably the tunneling current. Within this assumption the imaginary part of the phonon self-energy can be obtained directly from the known relationship $\Sigma^r - \Sigma^a = \Sigma^> - \Sigma^<$. In any case, the SCBA is valid in the small electron–phonon interaction limit and far from resonant situations where polaron effects should be taken into account.

Using the mathematical machinery described above, we have computed the tunneling current through an alkanethiolate molecule, $\text{Au}-\text{S}(\text{CH}_2)_8\text{S}-\text{Au}$. The Au atoms, composing the two contacts, are kept at fixed positions, corresponding to an ideal fcc crystal with Au–Au separations of 2.884 Å. First we relaxed the octanedithiol saturated with a hydrogen termination, on top of one Au surface comprising six atomic layers. After this first step we removed the hydrogen and put the second Au surface, taking care that the Au–S distance obtained at the first interface was reproduced at the second interface. Then we let this system relax again. Periodic boundary conditions are used in all these calculations. The final relaxed structure is shown in Figure 1.

Although we found that the global minima of the isolated octanedithiol is the highest symmetry configuration, the relaxed structure of the molecule attached to Au electrodes does not show any particular symmetry. The vibrational frequencies are slightly affected by this, since many degeneracies are broken. However, the differences in the whole spectrum are within 20%, which can be considered small and not relevant for the present analysis. The S atom is found to form a bond with an energy minimum at the hollow site of the Au(111) crystal. Actually, the exact minimal configuration is found with the sulfur atom slightly shifted from the hollow position, as reported in other ab initio DFT calculations.^{33,34} The S atom is found at 2.76 Å from the Au plane.

In Figure 2 the computed conductance and the $I-V$ characteristics of such system are reported. The theoretical

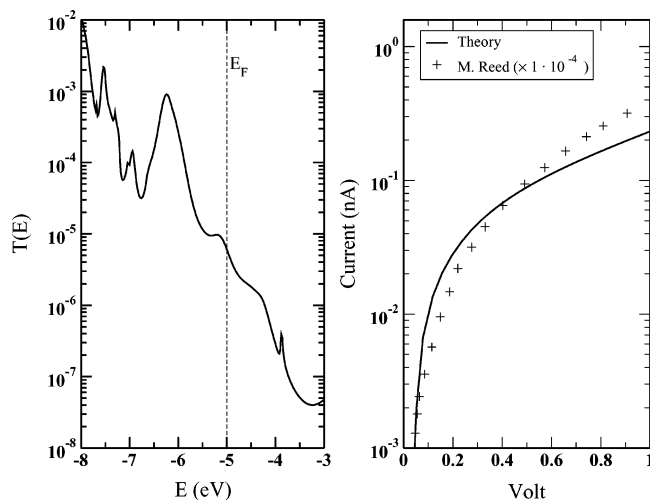


Figure 2. (left) Tunneling probability as a function of injection energy across a molecule of octanethiol. The Fermi energy corresponds to the Au contacts. (right) The computed I – V characteristics of the system (solid line) compared to recent experimental results (see text).

curve is also compared to recent experimental results,¹² obtained by measuring the current through a SAM assembled within a nanopore. Assuming that the SAM assembled in a lattice $R\sqrt{3} \times R\sqrt{3}$, from the measured nanopore diameter of 45 nm, we can estimate that approximately 10,000 molecules are sampled in parallel. Accordingly, the experimental measurements are scaled by a factor 10^{-4} in order to compare with our calculations. The order of magnitude of the tunneling current is predicted very well. This is important, particularly in relation to the absolute magnitude of the power dissipated in such system, as discussed later.

After the relaxation of the molecular coordinates, obtained by imposing the atomic forces to be smaller than 10^{-4} a.u., we proceeded to the computation of the vibrational modes and frequencies. For each of the 78 modes, we have computed the contribution to the inelastic current at $T = 0$ K and for an applied bias of 2 V. At $T = 0$, the incoherent part of the tunneling probability is related to the net phonon emission rate by $\tau^{-1} = I_{\text{inc}}/e$. This quantity is used as a measure of the electron–phonon strength and is used to compare the different modes. A summary of such computations is reported in Table 1 and in Figure 3a.

The lowest vibrational modes correspond to oscillations of the carbon atoms in the backbone plane, resembling the first harmonics of a string, and rigid twist around the C–C bonds of large subunits involving two or more CH_2 groups. The two sulfur atoms remain practically fixed or slide slightly over the Au surface. The frequencies of such modes are affected by large relative errors because they are sensitive to small differences in the atomic pair potentials and to the relaxed geometry. Furthermore, these modes are not easily accessible experimentally. We find that modes associated to internal twists of the C–C backbone involving the motion of $(\text{CH}_2)_2$ subunits are more effective in scattering electrons. As expected, the Au–S stretching modes, which are found in the range between 250 cm^{-1} to 320 cm^{-1} , in agreement with experiments,¹² give a large contribution to the electron–

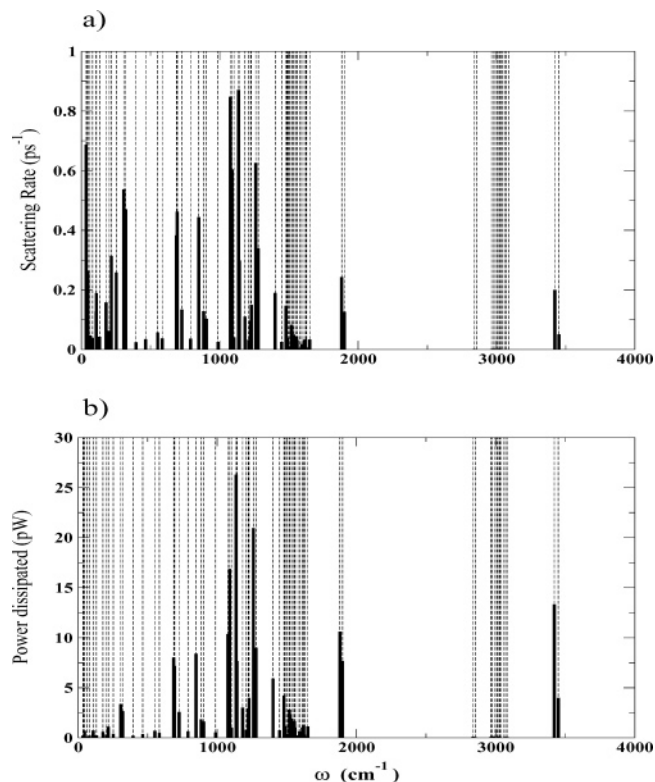


Figure 3. (a) Scattering rate and (b) power dissipated for each vibrational mode.

Table 1. Summary of the Most Important Frequencies (cm^{-1}) of the Octanethiol, Phonon Emission Rate (ps^{-1}), Followed by a Brief Description of the Mode and the Typical Experimental Value, Obtained by HREELS, Raman or IR¹²

ω	τ^{-1}	description	ω exp.
34.8	0.687	$(\text{CH}_2)_2$ twist	
106.9	0.127	$(\text{CH}_2)_2$ twist	
109.3	0.189	$(\text{CH}_2)_2$ twist	
178.8	0.157	$(\text{CH}_2)_2$ twist	
217.0	0.314	Au–S stretch	225–
320.6	0.470	Au–S stretch	–255
687.5	0.383	S–C stretch	650–706
693.6	0.462	S–C stretch	
848.1	0.444	CH_2 rock	715–925
1076.8	0.848	C–C stretch	1050
1136.2	0.871	C–C stretch	1120
1222.8	0.097	CH_2 wag	1300
1259.9	0.626	CH_2 twist	1250
1479.2	0.147	CH_2 twist	
1518.2	0.082	CH_2 scissor	1455
1881.0	0.243	CC+H swing	
2976.5	0.0024	C–H stretch.	2860
3421.4	0.200	H–Au stretch	

phonon scattering. Similarly, a large contribution is given by the C–S stretch modes, found around 690 cm^{-1} .¹² The band of modes found between 1000 and 1100 cm^{-1} corresponds to C–C stretch modes. These give the largest contribution to the incoherent current. A large contribution comes also from the modes related to motions of the CH_2 modes, particularly rocking and twisting. Wagging and scissoring modes, instead, give a smaller contribution.

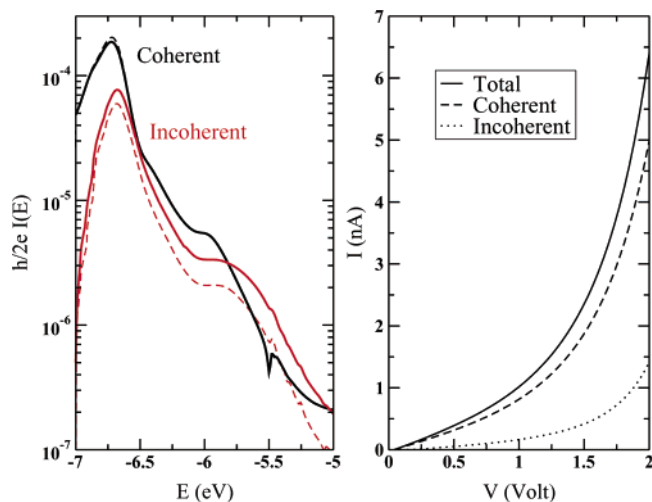


Figure 4. (left) Tunneling probability as a function of injection energy across a molecule of octanethiol. The contribution of the incoherent (dashed) and coherent (solid) tunneling current are shown. The black curves are the first-order BA, the red ones are the SCBA. (right) The SCBA I - V characteristics of the system.

In our analysis we also found non negligible signal from some modes that have not been discussed in experimental papers, since they are special to the Au/octanethiol/Au system and are not seen in isolated molecules. In particular, two modes around 1900 cm^{-1} (0.23 eV) are associated to a slight rotation of the C-S bond, a stretch of the C-C bonds involving the motion of the C at position 2, and a pronounced swing of the H atom closest to the Au surface. Another mode affecting the inelastic current is related to the oscillation of the hydrogens closest to the Au surfaces. Such modes could be seen as a Au-H stretch and are found at a frequency of $\approx 3400\text{ cm}^{-1}$ (0.42 eV).

The 34 modes giving an inelastic rate greater than 10^8 ps^{-1} have been included for the calculation of the incoherent current. Figure 4 shows the coherent and incoherent contributions to the total tunneling current resolved in energy for the bias of 2.0 V and the calculated I - V characteristics of the system.

The peaks in the transmission function correspond to features of the surface density of states of Au. In Figure 4 we have compared the first-order BA with the SCBA. It is important to remark that for this system the first-order Born approximation gives already an acceptable result and the SC loop does not introduce substantial changes in the transmission probability in the relevant energy range. Differences are appreciably deep in the energy gap, where the transmission probability is already small and the total contribution to the current is negligible. At this point it is possible to compute the amount of power dissipated in the molecule due to inelastic phonon emission. This calculation can be obtained by considering the virtual contact current, as discussed for instance in ref 35.

The power dissipated is given by the net rate of energy transferred to the molecule and can be easily calculated by

$$W = \frac{2}{h} \int_{-\infty}^{+\infty} \omega \text{Tr}[\Sigma_{\text{ph}}^<(\omega)G^>(\omega) - \Sigma_{\text{ph}}^>(\omega)G^<(\omega)] d\omega \quad (8)$$

This quantity is the virtual contact current, simply representing the total current scattered from its original energy to a new one after phonon emission (or absorption). This process can be associated to the concept of a phase-breaking contact which absorbs electrons at a given energy ($-I_{\text{ph}}(E)$) and emits them at another energy ($+I_{\text{ph}}(E)$). The net virtual current should be zero, for current conservation. From eq 8 we calculate that the power dissipated in the octanethiol is $W = 0.16\text{ nWatt}$ (1 eV/ps) at 2 V of applied bias.

It is interesting, however, to analyze the power dissipated in each vibrational mode, as shown in Figure 3b. This is not directly proportional to the emission rate, since the power dissipated depends on the phonon energy as well. As expected, the low frequency modes contribute little to the dissipation, despite the relatively large scattering rates. The modes giving the largest contribution are found in the band of C-C stretch modes, the C-S stretch, and the CH_2 rocking modes. Considerable power is also absorbed by the modes at 1900 and 3400 cm^{-1} , involving essentially movements of the hydrogens close to the Au surfaces.

The problem that needs to be addressed next is related to the dissipation of the absorbed heat, by coupling the vibrational modes to the environment. Computations of this kind, applied systematically to molecular bridges, allow the evaluation of molecular stability, assess the feasibility, and help the engineering of future molecular electronic devices.

Acknowledgment. We thank Dr. G. Fagas and Prof. G. Cuniberti for very useful discussions. R.G. thanks the Volkswagenstiftung for financial support.

References

- (1) Reed, M. A.; Chen, J.; Rawlett, A. M.; Price, D. W.; Tour, J. M. *Appl. Phys. Lett.* **2001**, *78*, 3735.
- (2) Xu, B.; Tao, N. J. *Science* **2003**, *301*, 1221.
- (3) Collier, C.; Wong, E. W.; Belohradsk, M.; Raymo, F. M.; Stoddart, J. F.; Kuekes, P. J.; Williams, R. S.; Heath, J. R. *Science* **1999**, *285*, 391.
- (4) Joachim, C.; Gimzewski, J. K.; Schittler, R. R.; Chavy, C. *Phys. Rev. Lett.* **1995**, *74*, 2102.
- (5) Metzger, R. M.; Chen, B.; Hopfner, U.; Lakshmikantham, M. V.; Vuillaume, D.; Kawai, T.; Wu, X. L.; Tachibana, H.; Hughes, T. V.; Sakurai, H.; Baldwin, J. W.; Hosch, C.; Cava, M. P.; Brehmer, L.; Ashwell, C. J. *J. Am. Chem. Soc.* **1997**, *119*, 10455.
- (6) Krezeminski, C.; Delerue, C.; Allan, G.; Vuillaume, D.; Metzger, R. M. *Phys. Rev. B* **2001**, *64*, 085405.
- (7) Wang, W.; Lee, T.; Reed, M. A. *Phys. Rev. B* **2003**, *68*, 035416.
- (8) Chen, Y.; Ohlberg, D. A. A.; Li, X.; Stewart, D. R.; Williams, R. S.; Jeppesen, J. O.; Nielsen, K. A.; Stoddart, J. F.; Olynick, D. L.; Anderson, E. *Appl. Phys. Lett.* **2003**, *82*, 1610.
- (9) Tour, J. M.; Zandt, L. V.; Husband, C. P.; Husband, S. M.; Wilson, L. S.; Franzon, P. D.; Nackashi, D. P. *IEEE Trans. Nanotech.* **2002**, *2*, 100.
- (10) Segal, D.; Nitzan, A. *J. Chem. Phys.* **2002**, *117*, 3915.
- (11) Chen, Y. C.; Zwolak, M.; Di Ventra, M. *Nano Lett.* **2003**, *3*, 1691.
- (12) Wang, W.; Lee, T.; Kretzschmar, I.; Reed, M. *Nano Lett.* **2004**, *4*, 643.
- (13) Kushmerick, J. G.; Lazorcik, J.; Patterson, C. H.; Shashidhar, R.; Seferos, D. S.; Bazan, G. C. *Nano Lett.* **2004**, *4*, 639.
- (14) Pecchia, A.; Latessa, L.; Di Carlo, A.; Lugli, P. *Physica E* **2003**, *19*, 139.
- (15) Pecchia, A.; Gheorghe, M.; Latessa, L.; Di Carlo, A.; Lugli, P. *IEEE Trans. Nanotech.* **2004**, *3*, 353.
- (16) Elstner, M.; Prezag, D.; Jugnickel, G.; Elsner, J.; Haug, M.; Frauenheim, T.; Suhai, S.; Seifer, G. *Phys. Rev. B* **1998**, *58*, 7260.
- (17) Porezag, D.; Frauenheim, T.; Kohler, T.; Seifert, G.; Kaschner, R. *Phys. Rev. B* **1995**, *51*, 12947.

- (18) Frauenheim, T. *Phys. Status Solidi B* **2000**, 271, 41.
- (19) Di Carlo, A.; Gheorghe, M.; Lugli, P.; Sternberg, M.; Seifert, G.; Frauenheim, T. *Physica B* **2002**, 314, 211.
- (20) Pecchia, A.; Di Carlo, A. *Rep. Prog. Phys.* **2004**, 67, 1.
- (21) Internet COmputing on DEMand, <http://icode.eln.uniroma2.it>.
- (22) Porezag, D.; Pederson, M. R.; Frauenheim, T.; Kohler, T. *Phys. Rev. B* **1995**, 52, 14963.
- (23) Seifert, G.; Porezag, D.; Frauenheim, T. *Int. J. Quantum Chem.* **1996**, 98, 185.
- (24) Mingo, N.; Makoshi, K. *Phys. Rev. Lett.* **2000**, 84, 3694.
- (25) Stokbro, K.; Hu, B. Y. K.; Thirstrup, C.; Xie, X. C. *Phys. Rev. B* **1998**, 58, 8038.
- (26) Emberly, E. G.; Kirczenow, G. *Phys. Rev. B* **2000**, 61, 5740.
- (27) Ness, H.; Fisher, A. J. *Chem. Phys.* **2002**, 281, 279.
- (28) Dong, B.; Cui, H. L.; Lei, X. L. *Phys. Rev. B* **2004**, 68, 205315.
- (29) Keldysh, L. V. *Sov. Phys. JEPT* **1965**, 20, 1018.
- (30) Kadanoff, L. P.; Baym, G. *Quantum Statistical Mechanics*; W. A. Benjamin: New York, 1962.
- (31) Galperin, M.; Ratner, M.; Nitzan, A. *Nano Lett.* **2004**, 4, 1605.
- (32) Haug, H.; Jauho, A. P. *Quantum Kinetics in Transport and Optics of Semiconductors*, Springer Series in Solid State Science; Springer: New York, 1993; vol. 123.
- (33) Yourdshahyan, Y.; Zhang, H. K.; Rappe, A. M. *Phys. Rev. B* **2001**, 63, 081405R.
- (34) Gottshlck, J.; Hammer, B. J. *Chem. Phys.* **2002**, 116, 784.
- (35) Datta, S. *Electronic Transport in Mesoscopic Systems*; Cambridge University Press: New York, 1995.

NL048841H